Formulas for time-lapse seismic refraction data analysis

Kris Innanen

ABSTRACT

Formulas for the analysis of time lapse seismic refraction difference data are derived, motivated by indications that during the 2014 University of Calgary Geophysics Field School a significant rain event produced detectable changes in the depth of the water table. The formulas are extensions of Hagedoorn's plus-minus method, wherein forward- and reverse-shot baseline and monitoring refraction travel times are mixed in several ways to extract differential depth-to-interface and jump in subsurface velocity values.

INTRODUCTION

Time lapse data analysis has benefited when it has had access to explanatory theories posed in terms of difference quantities (Landro, 2001; Ayeni and Biondi, 2010; Innanen et al., 2014). Motivated by this, we consider the problem of treating time-lapse refraction problems directly in terms of travel time differences in estimating quantities such as differential depth-to-interface and refraction velocity jumps.

Refraction methods are a powerful tool for the characterization of and correction for near-surface effects in exploration and monitoring seismology (Zuleta and Lawton, 2011). The P-wave velocity in the near surface can vary significantly, from day to day in response to for instance a rising water table after rain, or month to month with seasonal variability. We derive some relatively simple to use time lapse analysis formulas applicable to forward and reverse shot refraction data over regions where time lapse changes to the P-wave velocity or the depth and irregularity of interfaces have occurred. These are extensions to Hagedoorn's plus/minus method (Telford et al., 1990) wherein the summed and differenced first break picks are now constructed from combinations of baseline and monitoring data sets. Ultimately the interferometric interpretation of the standard plus/minus approach (Innanen, 2012) could be applied in their construction, but in the present paper we confine ourselves to formulas for analysis of arrival time picks.

The essential configuration is illustrated in Figure 1. In Figure 1a, two ray paths from the forward and reverse shots of the baseline survey are illustrated; in Figure 1b similar ray paths from the monitoring survey are illustrated. In Figures 1c-d two different time-lapse change parameters are illustrated. A change in the depth and/or shape of an interface is related to the time lapse change in the geophone delay time (Figure 1c) and the slope of the differential minus time is related to the time-lapse change in the velocity. Certain geophysical processes (e.g., rising water table) suggests a special case in which the interface changes but the velocity beneath the interface remains unchanged be considered also.

FORMULAS

The experimental variables x_g and L are defined as per Figure 2. In the forthcoming formulas, the delay times with the label g will refer to those which bear information from beneath the current (blue) geophone.

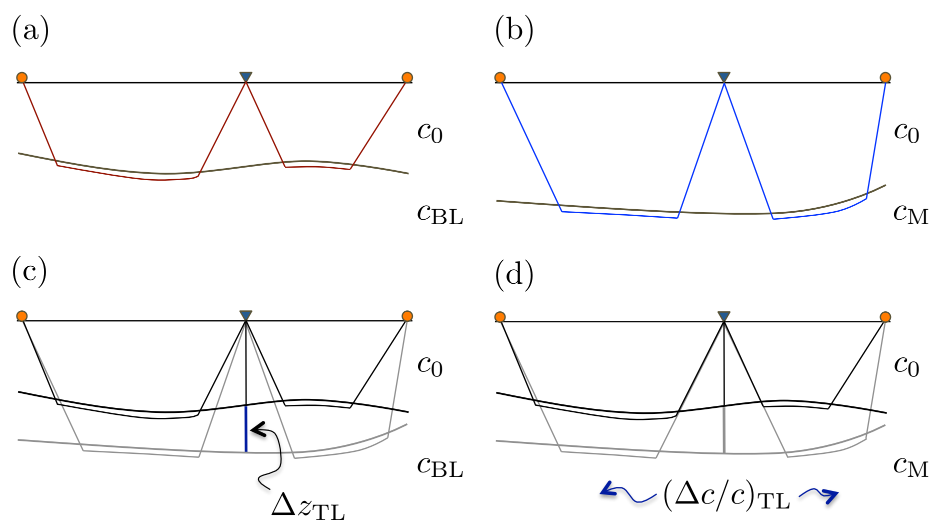

FIG. 1. Time lapse refraction configuration. (a) Forward (from left to right) and reverse (from right to left) shots into intermediate geophones support the plus-minus approach in a baseline survey; (b) and in a monitoring survey; (c) wherein differential geophone delay times are indicators of depth changes beneath the geophone; (d) and wherein slope changes derived from time-lapse minus times are indicators of velocity changes.

General time-lapse formulas

We set out the initial travel time formulas for the four arrival types illustrated in Figures 1a-b, making use of the source and receiver side delay times δ. The arrival times of a refracted wave from the forward and reverse shots during the baseline survey are given by

$$\tau_{\mathrm{BL}}^{\mathrm{F}} = \frac{x_g}{c_{\mathrm{BL}}} + \delta_{\mathrm{BL}}^{\mathrm{F}} + \delta_{\mathrm{BL}}^{\mathrm{g}}, \quad \tau_{\mathrm{BL}}^{\mathrm{R}} = \frac{L - x_g}{c_{\mathrm{BL}}} + \delta_{\mathrm{BL}}^{\mathrm{R}} + \delta_{\mathrm{BL}}^{\mathrm{g}}, \tag{1}$$

where c_{BL} is the velocity below the interface at the time of the baseline survey (c_{M} will be the velocity below the interface at the time of the monitoring survey). The superscripts refer to the forward (F) and reverse (R) configuration, the superscript g indicates it belongs to the current receiver, and the subscripts BL and (momentarily) M indicate which of the baseline or monitoring surveys the formula refers to. The monitoring counterparts are

$$\tau_{\mathrm{M}}^{\mathrm{F}} = \frac{x_g}{c_{\mathrm{M}}} + \delta_{\mathrm{M}}^{\mathrm{F}} + \delta_{\mathrm{M}}^{\mathrm{g}}, \quad \tau_{\mathrm{M}}^{\mathrm{R}} = \frac{L - x_g}{c_{\mathrm{M}}} + \delta_{\mathrm{M}}^{\mathrm{R}} + \delta_{\mathrm{M}}^{\mathrm{g}}. \tag{2}$$

Our versions of the plus and minus times will be made by interrelating the picks from the baseline and monitoring surveys:

$$\tau_{\mathrm{TL}}^{+1} = \tau_{\mathrm{M}}^{\mathrm{R}} + \tau_{\mathrm{BL}}^{\mathrm{F}} = \left(\frac{1}{c_{\mathrm{BL}}} - \frac{1}{c_{\mathrm{M}}}\right) x_g + \frac{L}{c_{\mathrm{M}}} + \delta_{\mathrm{M}}^{\mathrm{R}} + \delta_{\mathrm{BL}}^{\mathrm{F}} + \delta_{\mathrm{BL}}^{\mathrm{g}} + \delta_{\mathrm{M}}^{\mathrm{g}}, \tag{3}$$

mixes baseline forward with monitoring reverse shots, and

$$\tau_{\mathrm{TL}}^{+2} = \tau_{\mathrm{M}}^{\mathrm{F}} + \tau_{\mathrm{BL}}^{\mathrm{R}} = \left(\frac{1}{c_{\mathrm{M}}} - \frac{1}{c_{\mathrm{BL}}}\right) x_g + \frac{L}{c_{\mathrm{BL}}} + \delta_{\mathrm{BL}}^{\mathrm{R}} + \delta_{\mathrm{M}}^{\mathrm{F}} + \delta_{\mathrm{BL}}^{\mathrm{g}} + \delta_{\mathrm{M}}^{\mathrm{g}} \tag{4}$$

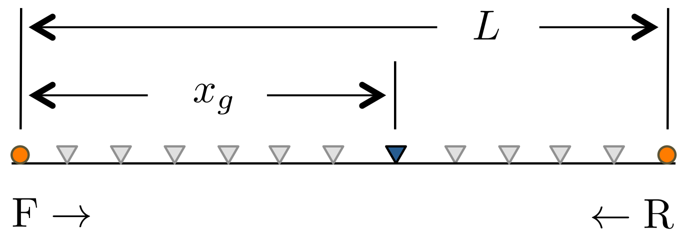

FIG. 2. Geophone location and source spread information variables in the context of the forward and reverse shots of the plus-minus method.

which mixes baseline reverse with monitoring forward shots. We can also define associated differences

$$\tau_{\mathrm{TL}}^{-1} = \tau_{\mathrm{BL}}^{\mathrm{F}} - \tau_{\mathrm{M}}^{\mathrm{R}} = \left(\frac{1}{c_{\mathrm{BL}}} + \frac{1}{c_{\mathrm{M}}}\right) x_g + \delta_{\mathrm{BL}}^{\mathrm{F}} + \delta_{\mathrm{BL}}^{\mathrm{g}} - \frac{L}{c_{\mathrm{M}}} - \delta_{\mathrm{M}}^{\mathrm{R}} - \delta_{\mathrm{M}}^{\mathrm{g}}, \tag{5}$$

and

$$\tau_{\mathrm{TL}}^{-2} = \tau_{\mathrm{M}}^{\mathrm{F}} - \tau_{\mathrm{BL}}^{\mathrm{R}} = \left(\frac{1}{c_{\mathrm{BL}}} + \frac{1}{c_{\mathrm{M}}}\right) x_g + \delta_{\mathrm{M}}^{\mathrm{F}} + \delta_{\mathrm{M}}^{\mathrm{g}} - \frac{L}{c_{\mathrm{BL}}} - \delta_{\mathrm{BL}}^{\mathrm{R}} - \delta_{\mathrm{BL}}^{\mathrm{g}}. \tag{6}$$

The plus times will be used first to determine time-lapse jumps $(\Delta c/c)_{\mathrm{TL}}$. Because

$$\frac{1}{c_{\mathrm{BL}}}\left(\frac{\Delta c}{c}\right)_{\mathrm{TL}} \approx \left(\frac{1}{c_{\mathrm{BL}}} - \frac{1}{c_{\mathrm{M}}}\right), \tag{7}$$

and

$$-\frac{1}{c_{\mathrm{BL}}}\left(\frac{\Delta c}{c}\right)_{\mathrm{TL}} \approx \left(\frac{1}{c_{\mathrm{M}}} - \frac{1}{c_{\mathrm{BL}}}\right), \tag{8}$$

if we define

$$\Delta\tau_{\mathrm{TL}}^{(1)} = \tau_{\mathrm{TL}}^{+1} - \tau_{\mathrm{TL}}^{+2} - \tau_{\mathrm{REC}}^{\mathrm{BL}} - \tau_{\mathrm{REC}}^{\mathrm{M}}, \tag{9}$$

and

$$\Delta\tau_{\mathrm{TL}}^{(2)} = \tau_{\mathrm{TL}}^{+1} + \tau_{\mathrm{TL}}^{+2} - \tau_{\mathrm{REC}}^{\mathrm{BL}} - \tau_{\mathrm{REC}}^{\mathrm{M}}, \tag{10}$$

where $\tau_{\mathrm{REC}}^{\mathrm{BL}}$ and $\tau_{\mathrm{REC}}^{\mathrm{M}}$ are the baseline and monitoring reciprocal times respectively. Then, by substituting in equations (7)–(8) we obtain

$$\Delta\tau_{\mathrm{TL}}^{(1)} = \frac{2}{c_{\mathrm{BL}}}\left(\frac{\Delta c}{c}\right)_{\mathrm{TL}} x_g + \text{constant}. \tag{11}$$

In other words, on a plot of $\Delta\tau_{\mathrm{TL}}^{(1)}$ vs x_g the slope is proportional to the time-lapse jump. Baseline properties having been determined, the jump is directly derivable from this slope. We also may take an interest in the differential receiver side delay time. The delay time at the monitoring survey $\delta_{\mathrm{M}}^{\mathrm{g}}$ can be written as a change from the delay time at the baseline survey $\delta_{\mathrm{BL}}^{\mathrm{g}}$:

$$\delta_{\mathrm{M}}^{\mathrm{g}} = \delta_{\mathrm{BL}}^{\mathrm{g}} + \delta_{\mathrm{TL}}, \tag{12}$$

in which case substituting equations (3) and (4) into equation (10), from which we obtain

$$\Delta\tau_{\mathrm{TL}}^{(2)} = 2(\delta_{\mathrm{M}}^{\mathrm{g}} + \delta_{\mathrm{BL}}^{\mathrm{g}}), \tag{13}$$

allows us to solve for the change in the delay time via

$$\delta_{\mathrm{TL}} = \frac{\Delta\tau_{\mathrm{TL}}^{(2)}}{2} - 2\delta_{\mathrm{BL}}^{\mathrm{g}}. \tag{14}$$

So, again provided we supply baseline information, through an adjusted version of the standard plus term solution for the depth of the interface beneath the geophone at x_g we determine the change in the depth beneath the geophone (refer to Figure 1):

$$\Delta z_{\mathrm{TL}}(x_g) \approx \frac{\delta_{\mathrm{TL}}(x_g)c_0}{\cos\theta_c}. \tag{15}$$

Structural time-lapse formulas

We lastly consider the important special case of a moving interface representing a change in velocities which do not themselves vary. A rising water table in unconsolidated near surface is an example of this. The basic equations are then simplified to

$$\tau_{\mathrm{BL}}^{\mathrm{F}} = \frac{x_g}{c} + \delta_{\mathrm{BL}}^{\mathrm{F}} + \delta_{\mathrm{BL}}^{\mathrm{g}}, \quad \tau_{\mathrm{BL}}^{\mathrm{R}} = \frac{L - x_g}{c} + \delta_{\mathrm{BL}}^{\mathrm{R}} + \delta_{\mathrm{BL}}^{\mathrm{g}}, \tag{16}$$

and

$$\tau_{\mathrm{M}}^{\mathrm{F}} = \frac{x_g}{c} + \delta_{\mathrm{M}}^{\mathrm{F}} + \delta_{\mathrm{M}}^{\mathrm{g}}, \quad \tau_{\mathrm{M}}^{\mathrm{R}} = \frac{L - x_g}{c} + \delta_{\mathrm{M}}^{\mathrm{R}} + \delta_{\mathrm{M}}^{\mathrm{g}}, \tag{17}$$

the main difference being that we invoke a single velocity c below the interface. The consequences to the formulas are simple — the slope of the $\Delta\tau_{\mathrm{TL}}^{(1)}$ vs x_g curve lapses to zero, and the structural formula remains the same. In fact when there is geological or other prior information suggesting that this special case is applicable, the "flatness" of the $\Delta\tau_{\mathrm{TL}}^{(1)}$ vs x_g curve will serve as a good indicator of the degree to which that is true.

CONCLUSIONS

We have provided some simple extensions to the Hagedoorn plus-minus formulas for the analysis of time-lapse forward and reverse shot refraction data. The outputs of these formulas in distinction from those of traditional plus-minus methods are time lapse difference quantities, $(\frac{\Delta c}{c})_{\mathrm{TL}}$ and $\Delta z_{\mathrm{TL}}(x_g)$. The quantities are derived using baseline quantities as input, which means standard refraction analysis must be carried out on the baseline data first. Of course, this raises the question *why not just do standard analysis on the monitoring data as well?* There is no theoretical answer to this question, which can be asked of most time lapse formulations, only practical and historical answers. It appears there is an interpretational benefit to solving directly for differences, or at least to having a framework in which we analyze difference quantities directly.

The plan forward is to have the 2014 University of Calgary Geophysics Field School refraction data, which was acquired across a significant rain event, subjected to analysis using these formulas to further assess their usefulness.

ACKNOWLEDGEMENTS

We thank the sponsors of CREWES for continued support. This work was funded by CREWES and NSERC (Natural Science and Engineering Research Council of Canada) through the grant CRDPJ 379744-08.

REFERENCES

Ayeni, G., and Biondi, B., 2010, Target-oriented joint least-squares migration/inversion of time-lapse seismic data sets: Geophysics, **75**, No. 3, R61–R73.

Innanen, K. A., 2012, Hagedoorn's +/- method and interferometric refraction imaging: CREWES Annual Report.

Innanen, K. A., Naghizadeh, M., and Kaplan, S. T., 2014, Perturbation methods for two special cases of the time-lapse seismic inverse problem: Geophysical Prospecting, **Published online**, doi: 10.1111/1365–2478.12,105.

Landro, M., 2001, Discrimination between pressure and fluid saturation changes from time-lapse seismic data: Geophysics, **66**, No. 3, 836–844.

Telford, W. M., Geldart, L. P., and Sheriff, R. E., 1990, Applied Geophysics: Cambridge University Press, 2nd edn.

Zuleta, L., and Lawton, D. C., 2011, P-wave and S-wave near-surface characterization in Nor theast British Columbia (NEBC): CREWES Annual Report.